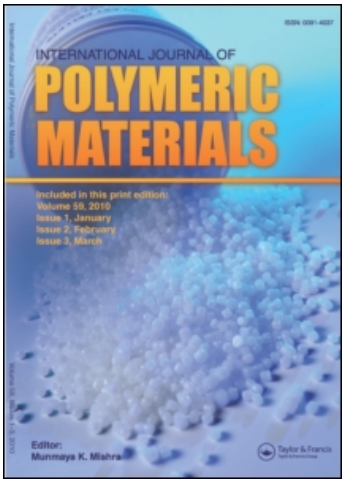


**International Journal of Polymeric Materials**
Publication details, including instructions for authors and subscription information:
http://www.informaworld.com/smpp/title~content=t713647664

# On the Fine Structure of Shish-Kebabs in Injection Moulded Polyethylene

J. Martínez-Salazar[a]; J. García Ramos[a]; J. Petermann[bc]
[a] Instituto de Estructura de la Materia, Madrid, Spain [b] Lehrstuhl fuer Werkstodtkunde, Dortmund University, Dortmund, Germany [c] Instituto de Optica, Madrid.

**To cite this Article** Martínez-Salazar, J. , Ramos, J. García and Petermann, J.(1993) 'On the Fine Structure of Shish-Kebabs in Injection Moulded Polyethylene', International Journal of Polymeric Materials, 21: 3, 111 — 121
**To link to this Article: DOI:** 10.1080/00914039308012038
**URL:** http://dx.doi.org/10.1080/00914039308012038

*Intern. J. Polymeric Mater.*, 1993, Vol. 21, pp. 111–121
Reprints available directly from the publisher
Photocopying permitted by license only

Printed in Malaysia

# On the Fine Structure of Shish-Kebabs in Injection Moulded Polyethylene

J. MARTÍNEZ-SALAZAR and J. V. GARCÍA RAMOS†

*Instituto de Estructura de la Materia, CSIC, Serrano 119.28006 Madrid, Spain*

and

J. PETERMANN

*Dortmund University, Lehrstuhl fuer Werkstodtkunde, FB Chemietechnik, Postfach 500 500, D4600 Dortmund, Germany*

*(Received October 18, 1992)*



The fine structure of melt-crystallized shish-kebabs is investigated by means of TEM, SAXS, DSC and RS. In addition to the well known two morphological entities (shish and kebab), a third entity called "transitional zone" has been detected by TEM and two independent SAXS maxima. The transitional zone is characterized by a crystal morphology somewhere in between the shish and kebab crystals and a comparatively high connectivity of molecules along those crystals. In situ SAXS experiments at elevated temperatures reveal the change of the size of this zone with crystallization conditions.

KEY WORDS Shish-kebab morphology, molecular connectivity, SAXS at elevated temperatures.

## 1. INTRODUCTION

Fibrous polyethylene (PE) crystals grown from stirred solutions have been intensively studied ever since the pioneering works of Pennings[1] and Mitsubashi.[2] It was soon recognized that the basic organization of the material was the well known shish-kebab structure where the shishs consist of crystallization-extended molecules and the kebabs of overgrown lamellae. The origin of this peculiar morphology, based on elongational stress-induced crystallization, was first postulated by Keller *et al.*[3] following previous work on extruded melts.[4] Morphological details of the shish-kebabs have been discussed by different authors.[5–10] It is now well-founded that shish and kebab crystals have different morphologies as well as thermal and mechanical properties.[11,12] Transmision electron microscopy (TEM) and small angle x-ray scattering (SAXS) indicate that the shish crystals which may exceed several

†Instituto de Optica 'Daza de Valdés', CSIC. Serrano, 121.28006 Madrid.

microns in length, are not perfect crystals with completely extended chains but rather they exist as alternating ordered and disordered regions.[5,9,13-16] Furthermore kebab crystals are proved to be lamellar crystals alike to ordinary melt-crystallized material.

An earlier independent work of Andrews[17] on stress-crystallized elastomers showed that a similar shish-kebab structure can be obtained under strain crystallization conditions from the melt. Analogous results were reported by Petermann *et al.*[18] in isostatic polystyrene. They also showed that overgrown lamellar crystals could be molten and recrystallized onto the fibrillar shish crystals. For pure shish crystals the authors demonstrated with dark field TEM and high resolution TEM that there exists a modulation of crystalline order along the shish crystals. More recently it has been proved that injection moulded material could give rise to interlocking shish-kebab structures.[19-23] The purpose of this paper is to present a more detailed description of the shish-kebabs structure for melt-crystallized injection moulded material by combining results from TEM, SAXS, DSC and Raman spectroscopy (RS) techniques.

## 2. EXPERIMENTAL



The sample investigated in this work is a commercial polyethylene (Lupolen 5261-Z, $M_w \approx 45 \times 10^4$) prepared by injection moulding. Details on sample preparation can be found in Reference 23. For TEM observations the sample was fractured at low temperature into two halves through a plane parallel to the mould axis and etched according to the method of Bassett *et al.*[24] Pt/C replicas from the clean surfaces were then mounted onto carbon coated grids. Ultrathin sections of the same part of the sample were also obtained at low temperature using a Reichert-Jung ultramicrotome. Before sectioning the sample was treated with chlorosulfonic acid according to earlier experiences[25] and the sections were stained with uranyl acetate. Thermograms were recorded in a Perkin Elmer DSC using a heating rate of 10 K/min. SAXS experiments were carried out using a Rigaku-Denki copper rotating anode operated at 12 kW. The oriented low angle patterns were recorded using a linear position sensitive counter with a space resolution of 100 μm at the counter. A modified Rigaku-Denki camera with pinhole collimation and a sample-counter distance of 1 m was employed. Heating experiments were performed by means of a Kratky heating cell. The temperature was monitored by a thermocouple placed inside the sample and close to the x-ray beam. Raman spectra of the sample were obtained using a Jobin Yvon Ramanor U-100 spectrometer in conjunction with the 514.5 nm line of a Spectra-Physics model 165 argon ion laser. The scattered light was collected in the direction perpendicular to the incident beam. Longitudinal acoustic modes (LAM) were identified on the spectra taken at room temperature.

## 3. RESULTS AND DISCUSSION

Figures 1(a) and (b) are the electron-micrographs of an etched-surface replica and of an ultrathin stained section of the sample, respectively. In both micrographs one

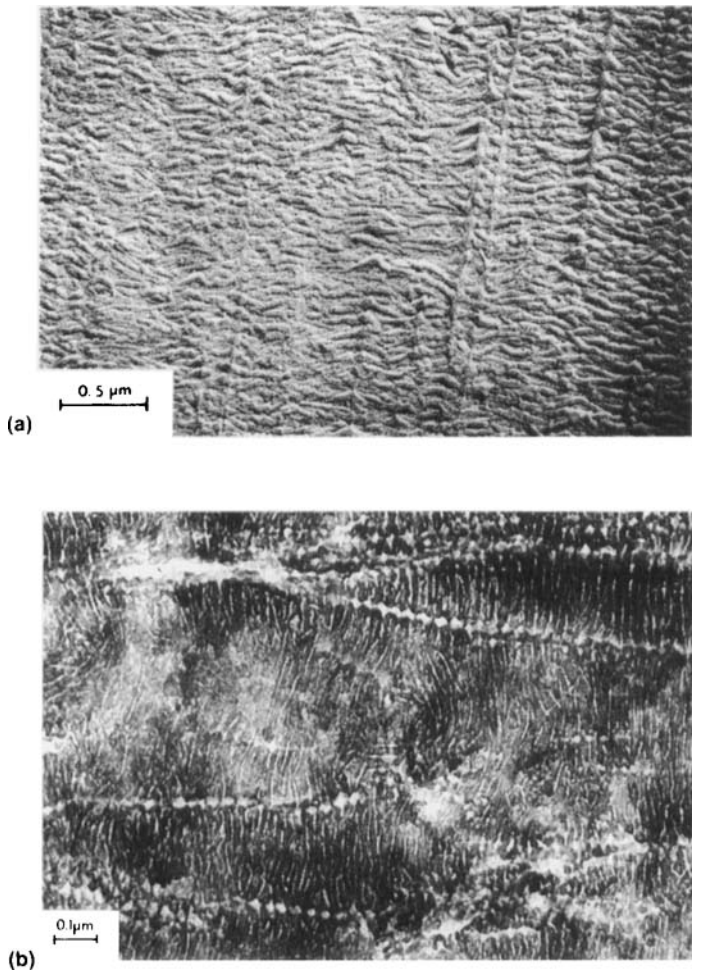


FIGURE 1 Transmission electron-micrographs of the investigated sample: (a) etched-surface replica, (b) ultrathin stained section.

can clearly distinguish shish and overgrown lamellar structures. One can also easily realize that the shish structure is not a continuous homogeneous entity but rather it varies in width at a very local scale. Lamellae attached to the shish crystals seem to have larger crystalline thickness than those further apart from the shish. In Figure 2 a simple sketch of the morphology is presented. In contrast to previous models a transition area between the core of the shish and the lamellar overgrowth is postulated. Melt crystallized shish kebabs may therefore consist out of three different entities: a) shish core, b) transition zone and c) lamellar overgrowth. The shish core is mainly characterized by a long range connectivity of the chains. It may also contain ordered and disordered regions, with the length of the former depending on growth conditions, flow gradient and molecular weight. They may even vary along a given shish crystal. In the transition zone molecules belong partially to the core and partially to the lamellar overgrowth. This means that

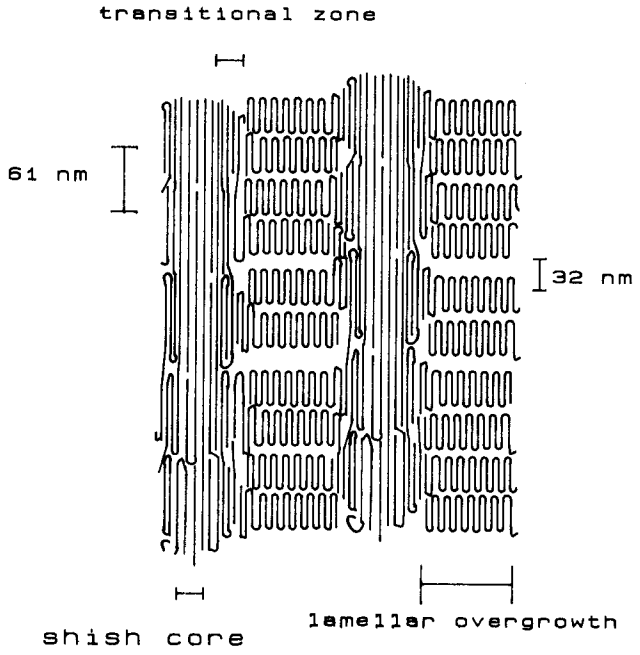


FIGURE 2 Sketch of the proposed shish-kebab structure including the shish core, the transitional zone and the overgrown lamella (kebabs).



connectivity along the orientation direction is somewhat lost. This transition zone could be identified as similar to the hairdressing zone of solution-grown shish kebabs.[8] Finally the lamellar region consist of more or less chain folded crystals implying therefore very low connectivity of the molecules along the orientation direction. The new feature of this model (transition zone) makes some relevant contributions to the overall morphology of the material. In what follows we shall use the term shish with the meaning of shish core plus its transition zone to the lamellar structure.

### 3.1. SAXS Results

A highly meridianal oriented X-ray diffraction low angle pattern is characteristic of this shish-kebab structure (see for instance Figure 6 in Reference 22). In this work the SAXS intensity have been recorded along the meridian through a 0.5 mm wide slit at the LPSC. In Figure 3(a) the SAXS trace of the as moulded material is presented. Here two different scattering maxima can be observed with Bragg spacing values of 32 nm and 61 nm, respectively. The lower spacing peak is not a second order maximum as it will be demonstrated later on. For our knowledge this is the first time that two independent small angle spacings are reported on shish kebab structures. Figure 3(b) shows the SAXS traces of the in situ heated sample. Annealing temperatures are indicated in each curve. For one trace the recording time was 200 s. The lower spacing peak starts to shift towards higher spacing values above 373 K while the inner peak remains in the same position up to 403 K. The

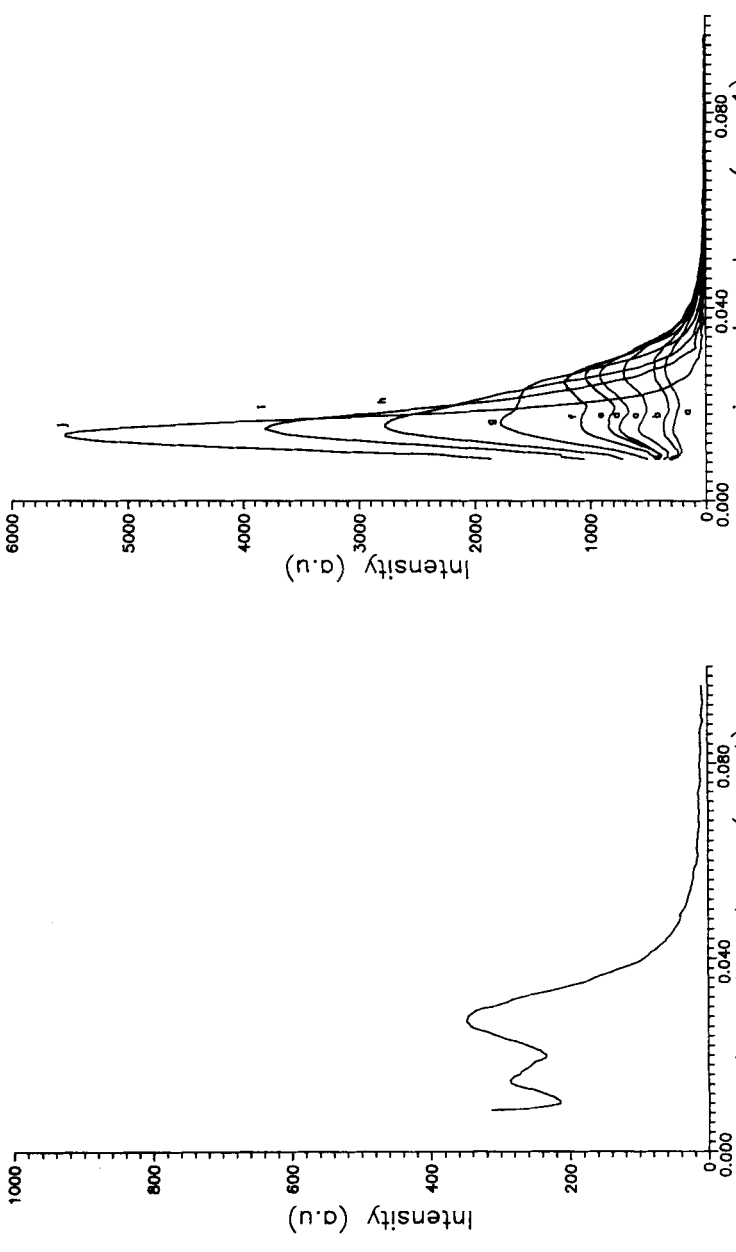


FIGURE 3 SAXS curves taken during the heating-cooling experiments: A) original sample at 293 K; B) heating at: 293 K (a), 333 K (b), 373 K (c), 383 K (d), 388 K (e), 393 K (f), 398 K (g), 401 K (h), 403 (i) and 406 K (j); C) cooling at: 406 K (j), 398 K (k), 395 K (l), 393 K (m), 373 K (n), 333 K (o) and 293 K (p); D) original (a) and recrystallized sample (b) at 293 K.

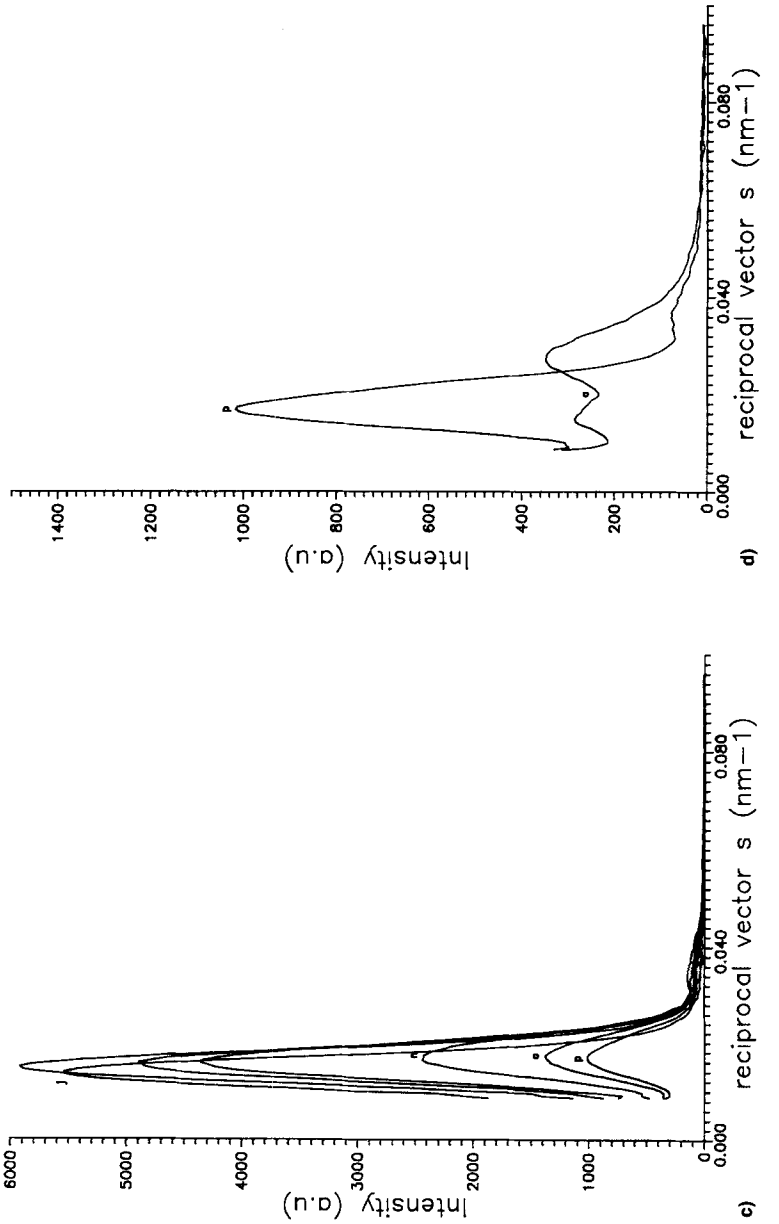


FIGURE 3 (*Continued*)

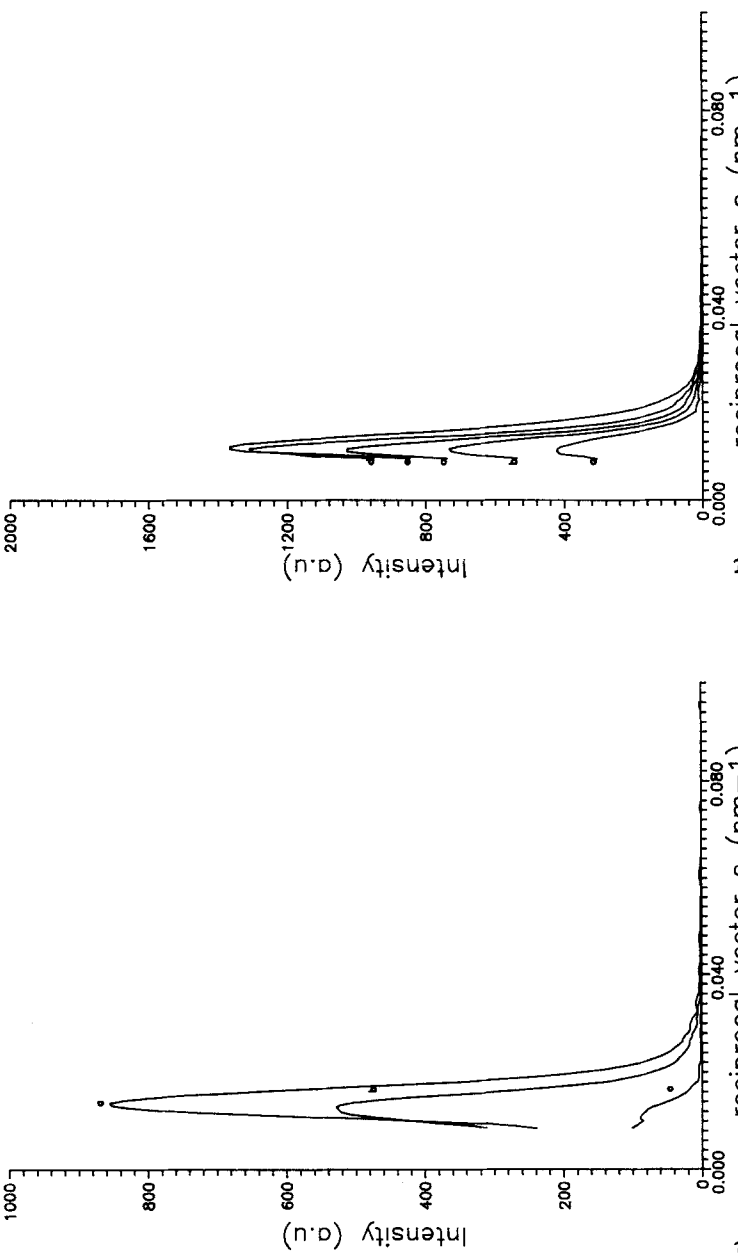


FIGURE 4 SAXS curves taken during: A) heating at: 406 K (a), 407 K (b) and 408 K (c); B) crystallization at 403 K for: 3 min (a), 5 min (b), 9 min (c), 15 min (d) and 180 min (e).

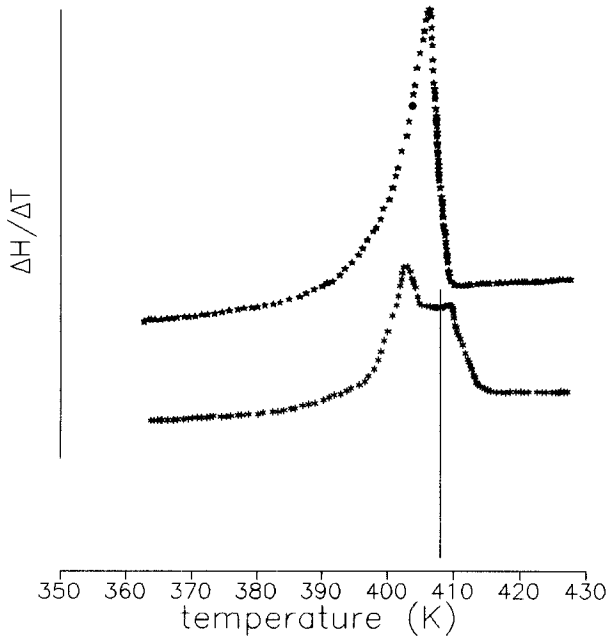


FIGURE 5 DSC traces showing the two melting maxima corresponding to the original sample (lower trace). The lower peak is associated to the melting of the overgrown lamellae while the higher one corresponds to the melting of the shishes. The upper trace corresponds to the melting of the recrystallized structure (see the electron-micrograph in Figure 7). Vertical line indicates the maximum annealing temperature during the SAXS experiments.



increase of the total scattered intensity can arise for one of several reasons, namely, increase in electron density differences between the phases, changes in crystallinity, higher perfection of the supermolecular structure, etc. However a detailed discussion of intensity variations of SAXS is not the subject of this paper. Nevertheless, we can draw some general conclusions when looking at the SAXS evolution above 393 K. The intensity of the higher spacing peak strongly increases with temperature while the second peak can hardly be seen. This implies that the low melting lamellar crystals have dissolved and recrystallized from the surface of the shish, enhancing the intensity of the higher spacing peak. On cooling (Figure 3(c)) the second peak does not reappear thus indicating that the new morphology consists out of shish crystals and lamellar crystals having both the same interphase periodicity. Figure 3(d) shows the SAXS traces of the sample before and after heat treatment. It is clear that after annealing most of the SAXS intensity is concentrated under the higher spacing peak and only a small fraction of the material, seemingly low molecular weight material, is diffracting at much lower spacing.

Figure 4(a) shows the SAXS traces recorded at extremely high annealing temperature. The SAXS intensity decreases drastically between 406 K and 408 K. Since the lamellar structure is expected to be molten at such a high temperature range (see the corresponding DSC trace on Figure 5), the intensity of the peak has to originate from the shish core regularity. Now if one drops the temperature to 403 K one can observe a rapid crystallization of the oriented lamellar morphology

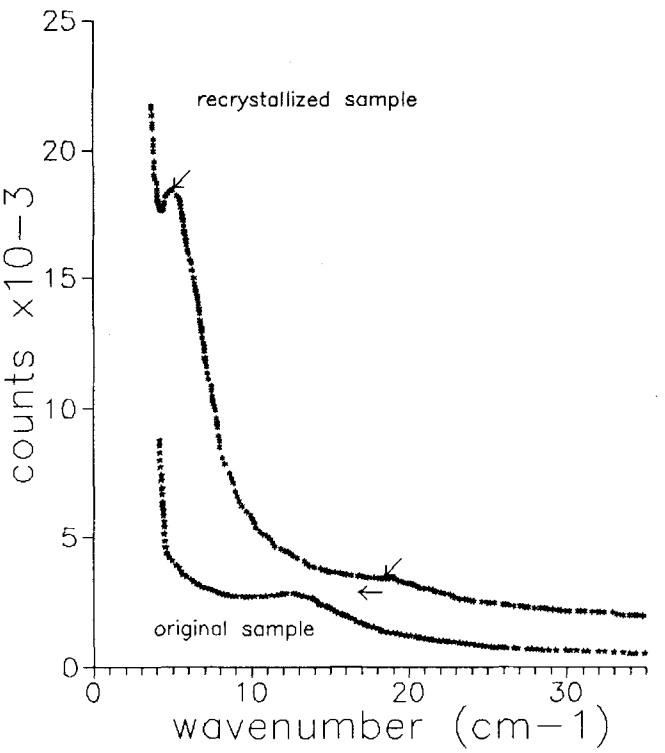


FIGURE 6 Raman spectra of the original and recrystallized samples. LAM modes of each sample are indicated by arrows.

(Figure 4(b)) which is monitored by the large increase in the SAXS intensity. The final Bragg spacing value is close to 100 nm which is of the order of the average distance of inhomogeneities along the shish core previously reported by other authors.[8,9]

### 3.2. Raman Results

Further information about crystal thickness has been obtained by RS. Figure 6 shows the characteristic LAM mode corresponding to the initial structure. It is worthwhile to mention that only the lamellar structure is giving rise to a well defined LAM peak. The frequency shift maximum is located at 11.5 $cm^{-1}$ corresponding to a lamellar thickness of ≈25 nm.[26] In the low frequency range ($\nu < 5.0$ $cm^{-1}$), where we would expect to detect the vibrating mode corresponding to the larger SAXS spacing, no LAM mode is observed. This result is linked to the fact that the molecules in the shish crystals have a long range connectivity in agreement with our proposed model. After the heat treatment described above the sample exhibits a lower LAM mode from which the derived lamellar thickness value (≈16 nm) is consistent with the long period determined from the outer SAXS maximum while the one corresponding to the original lamellar structure is shifted at higher frequency $\nu \approx 4.8$ $cm^{-1}$. This observation is in accordance with the explanation given to the SAXS results.

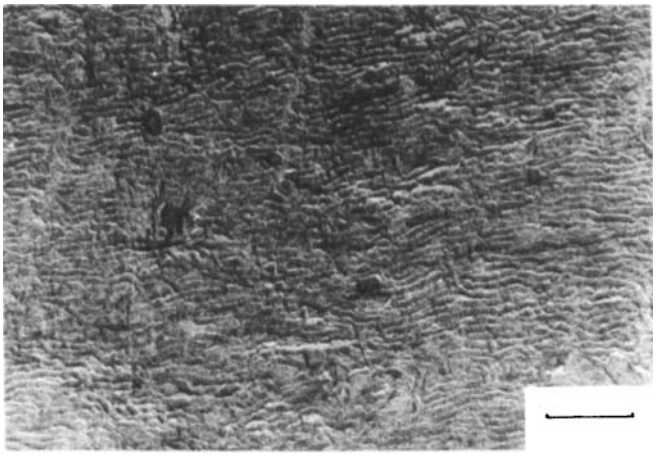

FIGURE 7 TEM replica of the etched-surface of the recrystallized sample. Note that the lamellar overgrowth masks entirely the shish structure (bar length = 0.5 μm).



The experimental results described throughout this paper support the model proposed at the beginning. It is clearly derived from the experiments that the morphology of the investigated sample consists of shish and lamellar structure. From the micrographs 1(a) and 1(b) shish core plus transitional zone can be clearly distinguished. As the transitional zone is part of the shish having less connectivity than the core itself, it is expected that upon annealing the transitional zone decreases in lateral size either by melting or by lateral growth of the core. After heat treatment of the sample the morphology of the shish is masked by the overgrowth of the lamellae. This implies that the transitional zone has rearranged during the heating process in such a way that it cannot longer be observed in the TEM micrographs (Figure 7). Note that the shish morphology is entirely masked by the lamellar overgrowth.

The presence of a transitional zone between the shish core and the lamellae provides a route to explain the mechanical behaviour, high strength, observed in materials containing this type of morphology. With our experiments we have proved that there is a connectivity between core of shish and lamellae, resulting in the reappearence of lamellar stacking even after high annealing temperature. Also the high rate of lamellar crystallization may be better understood with the existence of constrained transitional molecules. Furthermore, the observed branching of shishes can be explained by high shish nucleation rates (during processing) resulting from higher extension of the molecules close to a shish crystal (see Figure 1(b)).

In conclusion the existence of a transition zone is supported by TEM observations and high annealing temperature SAXS experiments. From a physical standpoint, there is clear distinction between the model of shish-kebabs consisting of pure shish core and overgrown lamellae and our model.

## Acknowledgment

Thanks are due to the CICYT (grant MAT90-0832) for the financial support of this work.

## References


1. A. J. Pennings and A. M. Kiel, *Kolloid Z. u. Z. Polymere*, **205**, 160 (1965).
2. S. Mitsubashi, *Bull. Text. Res. Inst. (Japan)*, **66**, 1 (1963).
3. A. Keller and M. J. Machin, *J. Macromol. Sci.*, **B1**, 41 (1967).
4. A. Keller, *J. Polym. Sci.*, **15**, 31 (1955).
5. A. J. Pennings, J. M. A. A. von der Mark and H. C. Booij, *Kolloid Z. u. Z. Polymere*, **236**, 99 (1970).
6. T. Nagasawa and Y. Shiromoura, *J. Polym. Sci. Polym., Phys. Ed.*, **12**, 2291 (1974).
7. D. T. Grubb and A. Keller, *Coll. & Polym. Sci.*, **256**, 218 (1978).
8. M. J. Hill, P. J. Barham and A. Keller, *ibid*, **258**, 1023 (1980).
9. D. T. Grubb and M. J. Hill, *J. Crystal Growth*, **48**, 321 (1980).
10. P. F. Van Hutten and A. J. Pennings, *J. Polym. Sci. Polym., Phys. Ed.*, **18**, 927 (1980).
11. P. J. Lemstra, C. W. M. Bastiaansen and H. E. H. Meijer Die Angew, *Makromol. Chem.*, **145/146**, 343 (1986).
12. A. J. Pennings, *Makromol. Chem., Suppl.*, **2**, 99 (1979).
13. P. J. Barham and A. Keller, *J. Mat. Sci.*, **20**, 2281 (1985).
14. M. Tsuji, A. Kemura, M. Ohara, A. Kawaguchi, K. Katayama and J. Petermann, *Seni-Gakkaishi*, **42**, T-580 (1986).
15. P. J. Barham, *Polymer*, **23**, 1112 (1982).
16. J. M. Schultz, J. Lin, R. Hendricks, J. Petermann and R. M. Gohil, *J. Polym. Sci.-Phys.*, **19**, 609 (1981).
17. A. J. Andrews, *Pro. Roy. Soc.*, **A277**, 562 (1964).
18. A. Petermann and H. Gleiter, *J. Polym. Sci., Polym. Lett. Ed.*, **B15**, 649 (1977).
19. Z. Bashir, J. A. Odell and A. Keller, *J. Mat. Sci.*, **19**, 3713 (1984).
20. Z. Bashir, J. A. Odell and A. Keller, *ibid*, **21**, 3992 (1986).
21. J. Martinez-Salazar, Abst. "Rolduc Polym. Metting," Rolduc (Holland), p. 41 (1987).
22. J. Martinez-Salazar, R. K. Bayer, T. A. Ezquerra and F. J. Balta Calleja, *Coll. & Polym. Sci.*, **267**, 409 (1989).
23. R. K. Bayer, T. A. Ezquerra, H. G. Zachmann, F. J. Balta Calleja, J. Martinez-Salazar, J. Meins, R. E. Diekow and P. Wiegel, *J. Mat. Sci.*, **23**, 475 (1988).
24. D. C. Bassett, *Principles of Polymer Morphology*, Cambridge University Press, Cambridge (1981).
25. J. Martinez-Salazar, A. Keller, M. E. Cagiao, D. R. Rueda and F. J. Balta Calleja, *Coll. & Polym. Sci.*, **261**, 412 (1983).
26. A. Peterlin, *J. Appl. Phys.*, **50**, 838 (1979).